Measurement of $D^{*\pm}$ diffractive cross sections in photoproduction at HERA

I.A.Korzhavina[*1]
(for the ZEUS Collaboration)

The first measurement of $D^{*\pm}$ meson diffractive photoproduction cross sections has been performed with the ZEUS detector at the HERA ep collider, using an integrated luminosity of $38\,\mathrm{pb}^{-1}$. The measurement has been performed for photon–proton center-of-mass energies in the range $130 < W < 280$ GeV and photon virtualities $Q^2 < 1$ GeV^2. $D^{*\pm}$ mesons have been reconstructed with $p_T^{D^*} > 2$ GeV and $-1.5 < \eta^{D^*} < 1.5$ from the decay channel $D^{*+} \to D^0\pi_s^+$ with $D^0 \to K^-\pi^+$ (+c.c.). The diffractive component has been selected with $0.001 < x_{I\!P} < 0.018$. The measured cross section in this kinematic range is: $\sigma^{diff}_{ep\to e'D^*Xp'} = 0.74 \pm 0.21(stat.)^{+0.27}_{-0.18}(syst.) \pm 0.16(p.diss.)$ nb (ZEUS preliminary). Measured integrated and differential cross sections have been compared to theoretical expectations.

[1] Institute of Nuclear Physics, Moscow State University, Russia
[*] email: irina@mail.desy.de

1 Introduction

Charm production processes are the ones which proceed mainly through gluon–initiated hard subprocesses and are perturbatively calculable. Thus, the diffractive production of charmed mesons can provide new tests of the partonic structure of diffractive interactions, in particular of their gluon component.

During the years of the HERA collider operation, integrated and differential cross sections for inclusive charm production were measured in kinematic ranges where an effective signal separation from suppressed backgrounds could be achieved [1,2]. The measured cross sections for photoproduction (PhP) and deep inelastic scattering (DIS) processes were compared with different next-to-leading (NLO) pQCD calculations. DIS data were found to be in good agreement with the calculations. The calculated PhP cross sections are lower than the measured ones, especially in the forward (proton) direction.

As for the diffractive charm production, there are only preliminary results on diffractive dissociation in DIS, measured with $D^{*\pm}$ mesons [3,4]. Here we present preliminary results on measurements by the ZEUS Collaboration of cross sections for diffractive photoproduction of $D^{*\pm}(2010)$ mesons[1] in the range of Pomeron fractional momentum $0.001 < x_{I\!P} < 0.018$ at energies $130 < W < 280$ GeV in the photon–proton center-of-mass frame and photon virtualities $Q^2 < 1$ GeV^2. D^* mesons were reconstructed through the decay channel $\mathrm{D}^{*+} \to \mathrm{D}^0\pi_s^+ \to (\mathrm{K}^-\pi^+)\pi_s^+$ (and c.c.) in the restricted kinematic region: $p_T^{D^*} > 2$ GeV and $|\eta^{D^*}| < 1.5$. Here $p_T^{D^*}$ is the D^* meson transverse momentum and $\eta^{D^*} = -\ln(\tan(\theta/2))$ is its pseudorapidity, defined in terms of the D^* polar angle θ with respect to the proton beam direction.

The measurements were performed at the HERA collider with the ZEUS detector, a detailed description of which can be found elsewhere [5]. The data were taken during 1996 and 1997, when HERA collided positron and proton beams with energies of 27.5 GeVand 820 GeV, respectively. An integrated luminosity of $38\,\mathrm{pb}^{-1}$ was used for this measure-

[1] In the following, $D^{*\pm}(2010)$ will be referred to simply as D^*.

ment. Charged particles were measured in the central tracking detector (CTD) [6]. To detect the scattered electron and to measure global energy values the uranium-scintillator sampling calorimeter (CAL) [7] was used. The luminosity was determined from the rate of the bremsstrahlung process $e^+p \to e^+\gamma p$, where the photon was measured by a lead scintillator calorimeter [8].

2 Kinematics of diffractive photoproduction

We consider diffractive photoproduction in ep scattering at HERA:

$$e(e) + p(p) \to e'(e') + X + p'(p'),$$

where the four-momenta of particles are shown in brackets. The collision occurs at the squared positron–proton center-of-mass energy $s = (e + p)^2$, and photon virtuality $Q^2 = -q^2$, where $q = e - e'$. The squared photon–proton center-of-mass energy $W^2 = (p + q)^2$ is defined for this reaction. One may consider that the interaction proceeds through a photon–Pomeron ($I\!P$) scattering:

$$\gamma(q) + I\!P(P_{I\!P}) \to X,$$

where $P_{I\!P} = p - p'$. This process is described by the invariant mass M_X of the hadronic system X, produced by photon dissociation, and the fraction of the proton momentum

$$x_{I\!P} = \frac{P_{I\!P} \cdot q}{p \cdot q} \simeq \frac{M_X^2}{W^2},$$

carried away by the Pomeron.

The variables W, M_X and $x_{I\!P}$ were reconstructed from the final hadronic system, measured by energy flow objects (EFO) [9], made from tracks detected by the CTD and from energy deposits in the CAL cells. The Jacquet–Blondel formula $W_{\text{JB}} = \sqrt{2E_p \sum_i (E - P_z)_i}$ [10] was used to reconstruct W. Here E_p is the proton beam energy. The invariant mass of the diffractively produced system M_X was calculated with the formula $M_X^2 = \left(\sum_i E_i\right)^2 - \left(\sum_i P_{x_i}\right)^2 - \left(\sum_i P_{y_i}\right)^2 - \left(\sum_i P_{z_i}\right)^2$. Sums in both equations run over energies E_i and momenta P_i of all EFOs. To select the

W range, $W_{\rm JB}$ was calculated with calorimeter cell deposits only so as to be consistent with the inclusive charm photoproduction analysis [1]. Measured values were corrected to the true ones by factors, determined from MC simulations of diffraction as average ratios of reconstructed to generated values. All variables were reconstructed to an accuracy of better than 15%.

3 Event selection and D^* reconstruction

Event selection and D^* reconstruction procedures are described in details elsewhere [1]. Here a short description is given.

Photoproduction events were selected by requiring that no scattered positron was identified in the CAL [11] and the photon–proton center-of-mass energy W is between 130 and 280 GeV. Under these conditions, the photon virtuality Q^2 is limited to values less than 1 GeV^2. The corresponding median Q^2 was estimated from a Monte Carlo (MC) simulation to be about 3×10^{-4} GeV^2. The D^* mesons were reconstructed through the decay channel $D^* \to (D^0 \to K\pi)\pi_s$ by combining candidates from charged tracks measured by the CTD. For the reconstruction, "right charge" track combinations, defined for $(K\pi)$ with two tracks of opposite charges and with a π_s having the charge opposite to that of the K meson in the $(K\pi)$, were accepted as long as the combination of invariant masses $\Delta M = M(K\pi\pi_s) - M(K\pi)$ and $M(K\pi)$ are within wide mass-windows around the nominal values of $\Delta M = M(D^*) - M(D^0)$ and $M(D^0)$ [12]. To determine the number of D^* mesons in the signal, combinatorial background was modelled by "wrong charge" track combinations and subtracted after normalization to the "right charge" distribution in the range $0.15 < \Delta M < 0.17$ GeV. "Wrong charge" combinations were defined for $(K\pi)$ with two tracks of the same charge and with a π_s of the opposite charge. The measurements were performed in the pseudorapidity range $-1.5 < \eta^{D^*} < 1.5$, where the CTD acceptance is high. The kinematic region in $p_T^{D^*}$ was limited to $2 < p_T^{D^*} < 8$ GeV.

The MC event samples used for this analysis were prepared with the RAPGAP [13], PYTHIA [14] and HERWIG [15] generators. Diffrac-

tive interactions were modeled in the framework of the resolved Pomeron model [16] with $\beta(1-\beta)$ or the H1 FIT2 [17] parametrisations for the initial partonic distributions in the Pomeron. Here β is the fraction of the Pomeron momentum carried by a parton, that couples to the Pomeron and participates in the hard interaction. The MRSG [18] and GRV-G HO [19] parametrisations were used for the proton and photon structure functions, respectively, when modelling non-diffractive interactions. The fragmentation of the generated partons (parton shower evolution and hadronisation) was simulated according to the LUND model [20] when using the RAPGAP or PYTHIA simulations. The HERWIG generator models the hadronisation process with a cluster hadronisation model. The MC events were processed through the standard ZEUS detector and trigger simulation programs and through the same event reconstruction package as was used for data processing. The shapes of MC and data distributions were found to be in reasonable agreement within statistical errors.

Diffractive events were identified by a large rapidity gap (LRG) between the scattered proton, which escaped detection through the beam pipe, and the hadronic system X, produced by the dissociated photon. The LRG events were searched for using the η_{max} method, for which η_{max} was defined as the pseudorapidity of the most forward EFO with energy greater than 400 MeV. Fig. 1 presents the η_{max} distribution for all photoproduced D^* mesons, reconstructed within the signal range $0.143 < M(K\pi\pi_s) - M(K\pi) < 0.148$ GeV and $1.80 < M(K\pi) < 1.92$ GeV after the combinatorial background subtraction. This distribution shows two structures. The plateau-like structure at $\eta_{max} \lesssim 2$ is populated predominantly by the LRG events, while the wide peak-like structure around $\eta_{max} \sim 3.5$ originates from the non-diffractive events and has an exponential fall-off towards lower values of η_{max}. From a comparison between the data points and a sum of simulated diffractive and non-diffractive event distributions, normalised to the data, a cut-off of $\eta_{max} = 1.75$ was chosen as a compromise between the magnitudes of the diffractive signal and the non-diffractive background. The non-diffractive background fractions for subtraction were estimated from the MC-to-data distribution ratios, using non-diffractive MC simulations.

When using the η_{max} method for diffractive event selection, one needs

to take into account the following properties of the method. The measurement of rapidities by the CAL is limited to the edge of the forward beam hole of the CAL. Thus the proton dissociative events, $ep \to e'XN$, can satisfy the requirement $\eta_{max} < 1.75$ if the proton dissociative hadronic system N has invariant mass small enough to pass undetected through the forward beam pipe. It was found earlier that the proton dissociation contribution comprises 0.31 ± 0.15 [21]. Measured cross sections were corrected for this value. A cut in η_{max} correlates with a range of accessible $x_{I\!P}$ values. $\eta_{max} < 1.75$ restricts $x_{I\!P} < 0.018$. In addition, limited acceptance restricts $x_{I\!P} > 0.001$.

After the above selection and the "wrong charge" background subtraction a signal of 56 ± 10 diffractively photoproduced D^* mesons was found in the ΔM distribution (Fig.2).

4 Cross sections

The inclusive D^* production cross section is given by:

$$\sigma_{ep\to D^*X} = \frac{N^{corr}_{D^*}}{\mathcal{L} \cdot B_{D^*\to(D^0\to K\pi)\pi}} \ ,$$

where $N^{corr}_{D^*}$ is the number of observed D^* mesons corrected for the acceptance, $\mathcal{L} = 38.0 \pm 0.6$ pb^{-1} is the integrated luminosity and $B_{D^*\to(D^0\to K\pi)\pi} = 0.0263 \pm 0.0010$ is the combined $D^* \to (D^0 \to K^+\pi^-)\,\pi_s$ decay branching ratio [12]. Acceptance corrections were calculated using the RAPGAP MC sample.

The total D^* diffractive photoproduction cross section in the kinematic region $Q^2 < 1$ GeV^2, $130 < W < 280$ GeV, $p_T^{D^*} > 2$ GeV, $|\eta^{D^*}| < 1.5$ and $0.001 < x_{I\!P} < 0.018$ was measured to be
$\sigma^{diff}_{ep\to e'D^*Xp'} = 0.74 \pm 0.21(stat.)^{+0.27}_{-0.18}(syst.) \pm 0.16(p.diss.)$ nb (ZEUS preliminary). The last error is due to the uncertainty in the proton dissociative background subtraction. Other sources of systematic uncertainties due to analysis and detector features were studied and their effect on the cross section was estimated. The largest contributions to the systematic error came from the CAL energy scale uncertainty ($^{+12.0}_{-4.8}\%$), the signal determination procedure ($^{+16.4}_{-14.5}\%$), the selection of diffractive events ($^{+11.3}_{-8.0}\%$) and

the acceptance correction calculations ($^{+26.5}_{-16.9}\%$). The overall normalisation uncertainties due to the error in the luminosity value ($\pm 1.7\%$) and in the D^* and D^0 decay branchings ($\pm 3.8\%$) were not included in the systematic error quoted above. All of the systematic uncertainties were added in quadrature to determine the overall systematic uncertainty of $^{+35.6}_{-24.1}\%$. The summation of the systematic uncertainties was also performed for each bin of the differential distributions.

The measured D^* diffractive photoproduction cross section, while only a fraction of the total diffractive contribution, amounts $\sim 4\%$ of the inclusive D^* photoproduction cross section, $\sigma_{ep\to D^*X} = 18.9 \pm 1.2(stat)^{+1.8}_{-0.8}(syst)$ nb [1], measured in the same kinematic range. This fraction indicates that diffractive charm production is not suppressed as much as some early models predicted [22].

Measurements were compared to resolved Pomeron model expectations [16], calculated with the RAPGAP Monte Carlo program in the same kinematic region. Partonic distributions in the Pomeron were parametrised by the fit to the HERA data [17], performed by H1 Collaboration (H1 FIT2). Only the BGF mechanism of charm production was accounted for. The leading order RAPGAP Monte Carlo, with the H1 FIT2 Pomeron parametrisation, predicts 1.42 nb for the D^* diffractive photoproduction cross section in the same kinematic range [23].

Differential cross sections for $d\sigma/dp_T^{D^*}$, $d\sigma/d\eta^{D^*}$, $d\sigma/dM_X$ and $d\sigma/dx_{I\!P}$ are presented in Figs. 3–6. All of the above mentioned systematic uncertainies were added in quadratures with statistical errors (inner error bars) in each bin to calculate the total error (outer error bars), both of which are shown in Figs. 3–6.

The measured differential cross sections (Figs. 3–6), when compared to the ones of the resolved Pomeron model calculated with the RAPGAP MC program show reasonable agreement in shape with the theoretical expectations considering the measurement errors. $d\sigma/dp_T^{D^*}$ agrees well and the other three distributions are shifted somewhat to larger values with respect to the predictions.

5 Summary and conclusions

The first measurement of diffractive D^* photoproduction has been performed with the ZEUS detector at HERA with a luminosity of $38\,\mathrm{pb}^{-1}$. The preliminary results are reported here. The total D^* diffractive photoproduction cross section in the kinematic region $Q^2 < 1$ GeV^2, $130 < W < 280$ GeV, $p_T^{D^*} > 2$ GeV, $|\eta^{D^*}| < 1.5$ and $0.001 < x_{I\!P} < 0.018$ is measured to be $\sigma^{diff}_{ep\to e'D^*Xp'} = 0.74 \pm 0.21(stat.)^{+0.27}_{-0.18}(syst.) \pm 0.16(p.diss.)$ nb (ZEUS preliminary) . The leading order calculations in the framework of the resolved Pomeron model predict 1.42 nb for this cross section. The differential cross section shapes for $d\sigma/dp_T^{D^*}$, $d\sigma/d\eta^{D^*}$, $d\sigma/dM_X$ and $d\sigma/dx_{I\!P}$ show reasonable agreement with the resolved Pomeron model considering the measurement errors.

6 Acknowledgements

We would like to thank the DESY Directorate for their strong support and encouragement. The remarkable achievements of the HERA machine group were essential for this work and are greatly appreciated. We would like to thank H.Jung for fruitful discussions and help in the use of the RAPGAP MC generator.

References

[1] ZEUS Collaboration (M.Derrick *et al.*), Phys. Lett. B **349**, 225(1995); ZEUS Collaboration (J.Breitweg *et al.*), Phys. Lett. B **401**, 192(1997); Phys. Lett. B **407**, 402(1997); Eur. Phys. J. C **6**, 67(1999); Eur. Phys. J. C **12**(1), 35(2000).

[2] H1 Collaboration (S.Aid *et al.*), Nucl. Phys. B **472**, 32(1996); Z. Phys. C **72**, 593(1996); H1 Collaboration (C. Adlof *et al.*), Nucl. Phys. B **545**, 21(1999).

[3] ZEUS Collaboration (paper N-645), *Int. Europhys. Conf. on High Energy Physics, Jerusalem, Israel,1997*; ZEUS Collaboration, (paper N-

527), *Int. Europhys. Conf. on High Energy Physics, Tampere, Finland,1999*; ZEUS Collaboration *8th International Workshop on Deep-Inelastic Scattering DIS2000, Liverpool, England, 2000*; ZEUS Collaboration (abstract 874), *the XXXth Int. Conf. on High Energy Physics, Osaka, Japan, 2000.*

[4] H1 Collaboration (pa02-60), *28th Int. Conf. on High Energy Physics, Warsaw, Poland, 1996*; H1 Collaboration, *29th Int. Conf. on High Energy Physics ICHEP98, Vancouver, Canada, 1998*; H1 Collaboration, *8th International Workshop on Deep-Inelastic Scattering DIS2000, Liverpool, England, 2000.*

[5] ZEUS Collaboration (M.Derrick *et al.*), Phys. Lett. B **293**, 465(1992); The ZEUS detector: Status Report 1993, DESY, 1993.

[6] N.Harnew *et al.*, Nucl. Instrum. Methods A **279**, 290(1989); B.Foster *et al.*, Nucl. Phys. Proc. Suppl. B **32**, 181(1993), Nucl. Instrum. Methods A **338**, 254(1994).

[7] M.Derrick *et al.*, Nucl. Instrum. Methods A, **309**, 77(1991); A.Andresen *et al.*, ibid., 101(1991); A.Caldwell *et al.*,Nucl. Instrum. Methods, A **321**, 356(1992); A.Bernstein *et al.*, Nucl. Instrum. Methods, A **336**, 23(1993).

[8] J.Andruszków *et al.*, DESY 92-066, 1992; ZEUS Collaboration (M.Derrick *et al*)., Z. Phys. C **63**, 391(1994); Nucl. Phys. B **303**, 634(1988).

[9] ZEUS Collaboration (M.Derrick *et al.*), Eur. Phys. J. C **1**, 81(1998); Eur. Phys. J. C **6**, 43(1999); G.Briskin, PhD Thesis, University of Tel Aviv, 1998.

[10] F.Jacquet and A.Blondel, *Proc. of the Study for an ep Facility for Europe*, DESY 79-48, 391(1979).

[11] ZEUS Collaboration (M. Derrick *et al.*), Phys. Lett. B **322**, 287(1994).

[12] C. Caso *et al.*, Particle Data Group, Eur. Phys. J. C **3**, 1(1998).

[13] H.Jung, Comp. Phys. Comm. **86**, 147(1995).

[14] T. Sjöstrand, Comp. Phys. Comm. **82**, 74(1994).

[15] G.Marchesini *et al.*, Comp. Phys. Comm. **67**, 465(1992).

[16] G.Ingelman and P.Schlein, Phys. Lett. B **152**, 256(1985);
A.Donnachie and P.V.Landshoff, Nucl. Phys. B **303**, 634(1988).

[17] H1 Collaboration (C.Adloff *et al.*), Z. Phys. C **76**, 613(1997).

[18] A.D. Martin, W.J. Stirling, and R.G. Roberts, Phys. Lett. B **354**, 155(1995).

[19] M. Glück, E. Reya, and A. Vogt, Phys. Rev. D **46**, 1973(1992).

[20] T. Sjöstrand, Comp. Phys. Comm. **39** 347(1986);
T. Sjöstrand and M.Bengtsson, Comp. Phys. Comm. **43**, 367(1987).

[21] ZEUS Collaboration (J.Breitweg *et al.*), Phys. Lett. B **315**, 43(1999);
Eur. Phys. J. C **1**, 81(1998).

[22] N.N.Nikolaev and B.G.Zakharov, Z. Phys. C **53**, 331(1992).

[23] H.Jung, private communication.

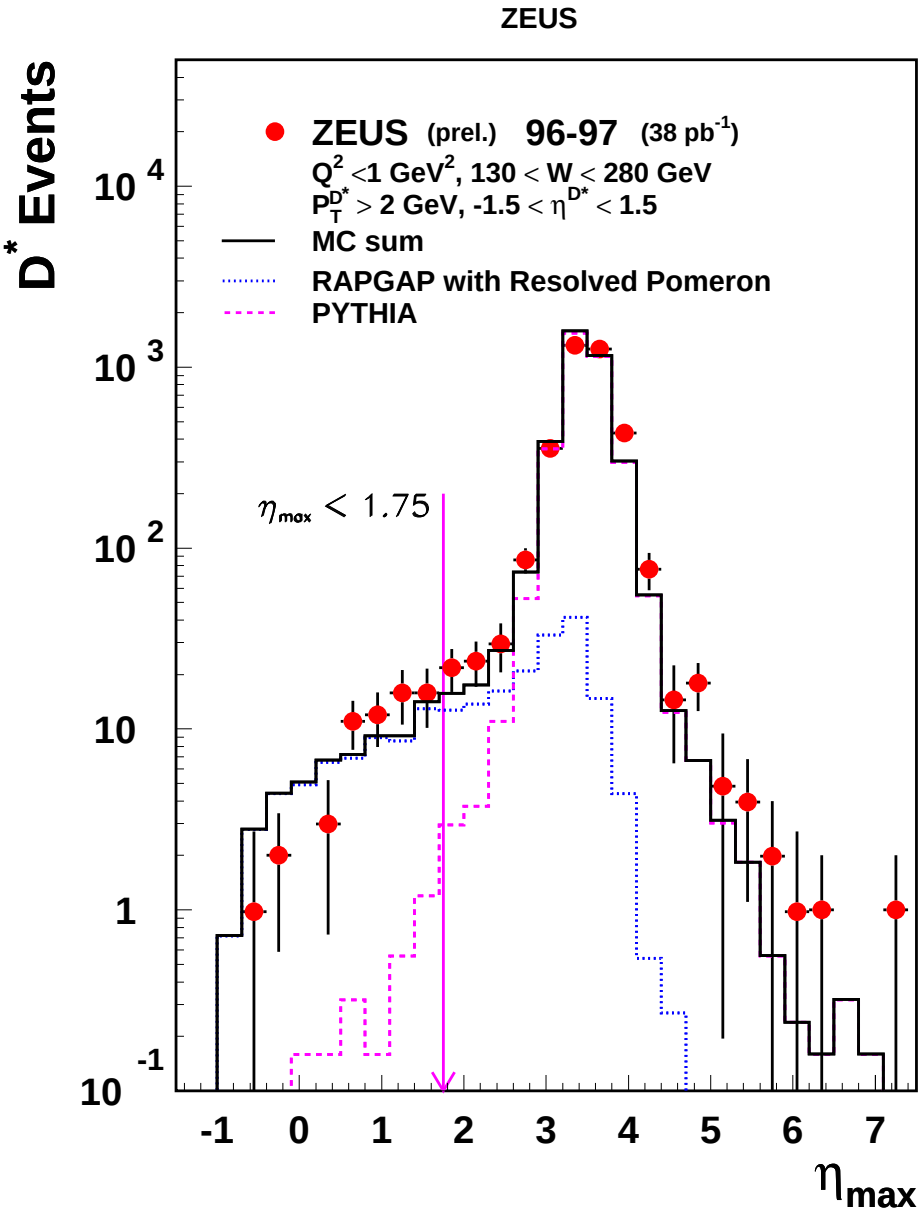

Figure 1: *Comparison of the measured η_{max} distribution (dots) with the sum of the diffractive and non-diffractive MC distributions (histograms) for events with D^* mesons. D^* candidates were selected in the kinematic region $Q^2 < 1\ GeV^2$, $130 < W < 280\ GeV$, $p_T^{D^*} > 2\ GeV$ and $|\eta^{D^*}| < 1.5$. Sum distribution of the diffractive resolved Pomeron RAPGAP MC (dotted histogram) and non-diffractive MC (dashed histogram) events were normalised to have the same area as the data distribution.*

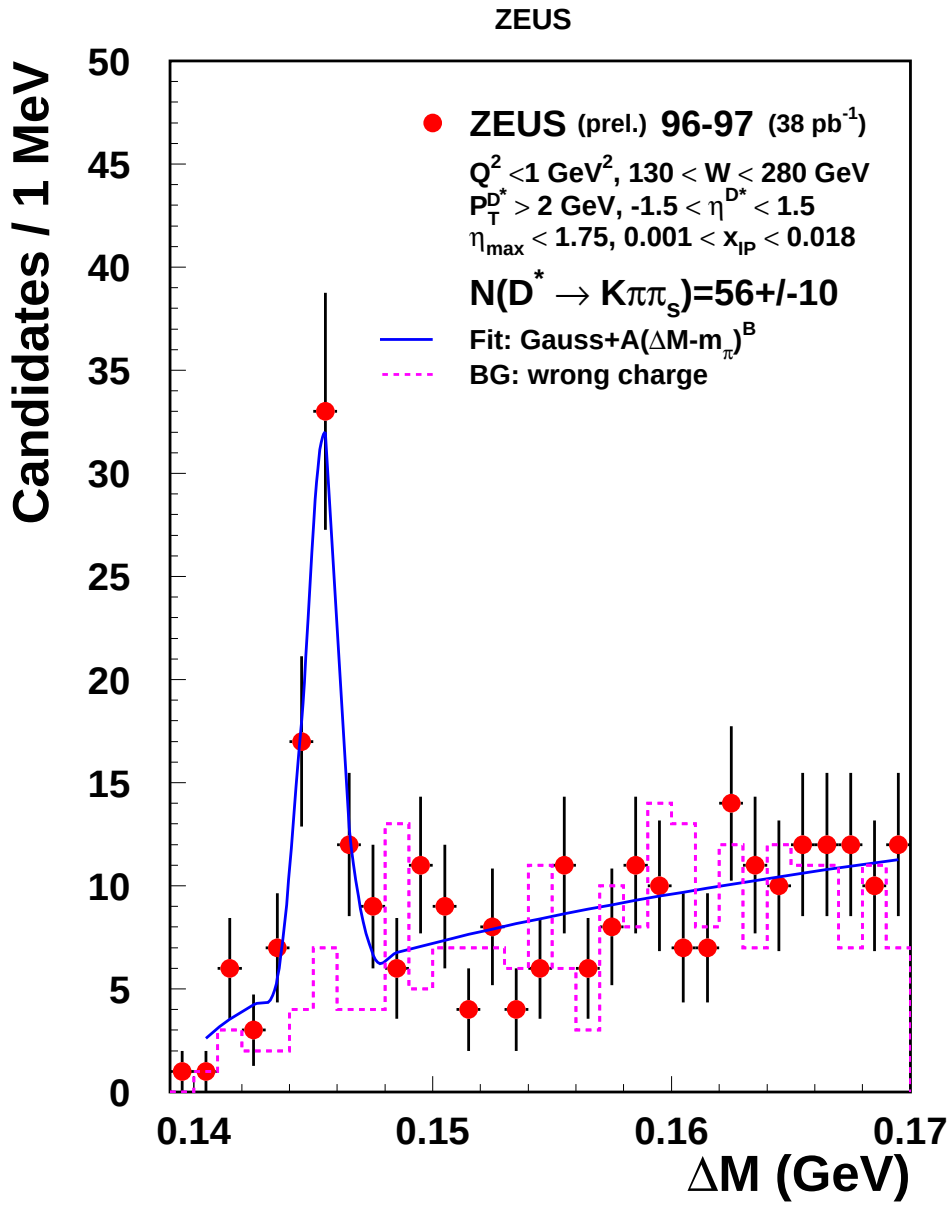

Figure 2: *The ΔM distribution for the D^* diffractive photoproduction reaction with $D^* \to (D^0 \to K\pi)\pi_s$ for $Q^2 < 1\ GeV^2$, $130 < W < 280\ \ GeV$ and $0.001 < x_{I\!P} < 0.018$. The kinematic range of measurements is $p_T^{D^*} > 2\ GeV$ and $|\eta^{D^*}| < 1.5$. The dots are for the right charge combinations, and the dashed histogram is for the wrong charge combinations from the D^0 signal region (1.80 - 1.92 GeV). The full line is the result of a fit to a sum of a Gaussian and the functional form $A(\Delta M - m_\pi)^B$.*

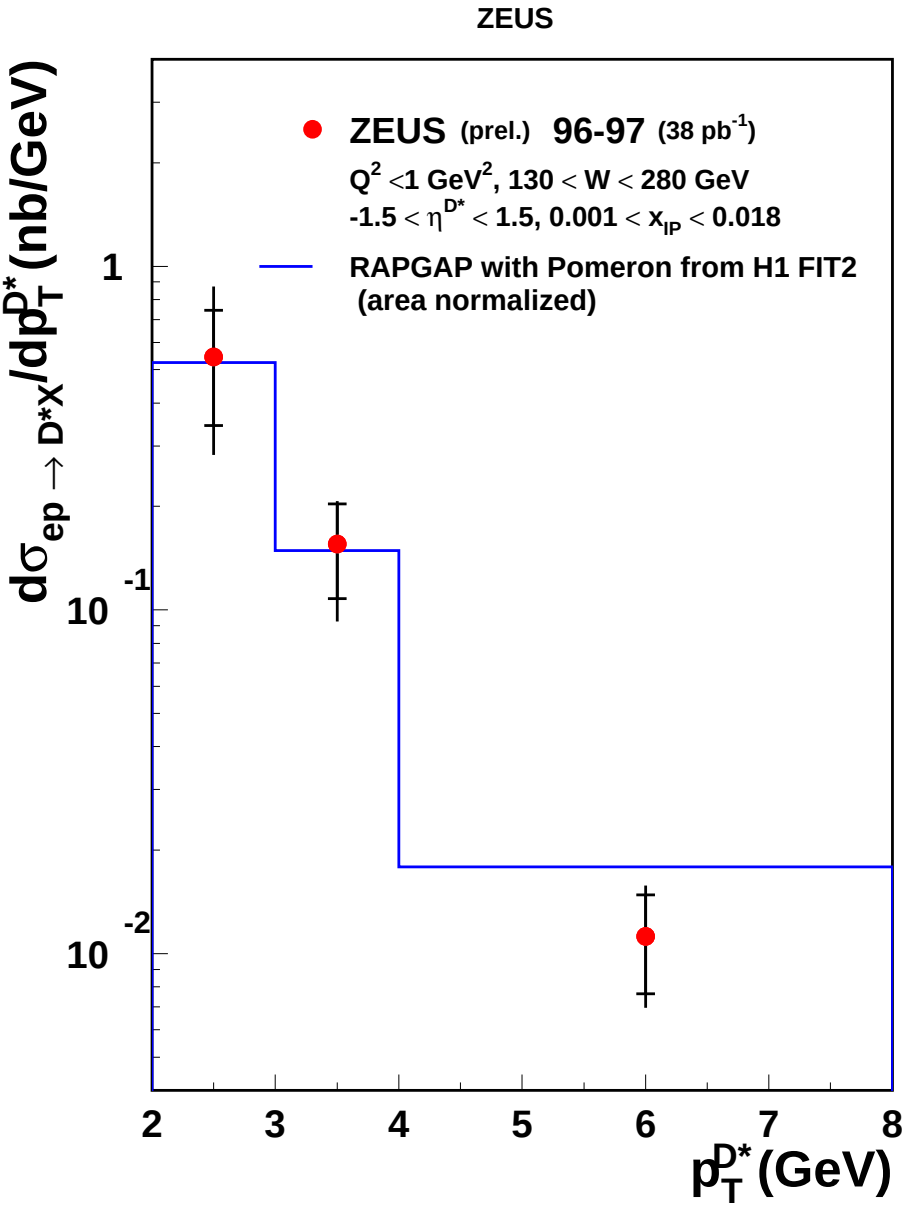

Figure 3: *Differential cross section $d\sigma/dp_T^{D^*}$ (dots) for the diffractive photoproduction reaction $ep \to e' D^* X p'$ for $Q^2 < 1\ GeV^2$, $130 < W < 280\ GeV$ and $0.001 < x_{I\!P} < 0.18$. The kinematic range of measurements is $p_T^{D^*} > 2\ GeV$ and $|\eta^{D^*}| < 1.5$. The inner bars show the statistical errors, and the outer bars correspond to the statistical and systematic errors, added in quadrature. The data are compared with the distributions of the RAPGAP MC diffractive events, simulated in the framework of the resolved Pomeron model with the H1 FIT2 Pomeron parametrization (histogram). The MC distribution has been normalized to have the same area as the data distribution.*

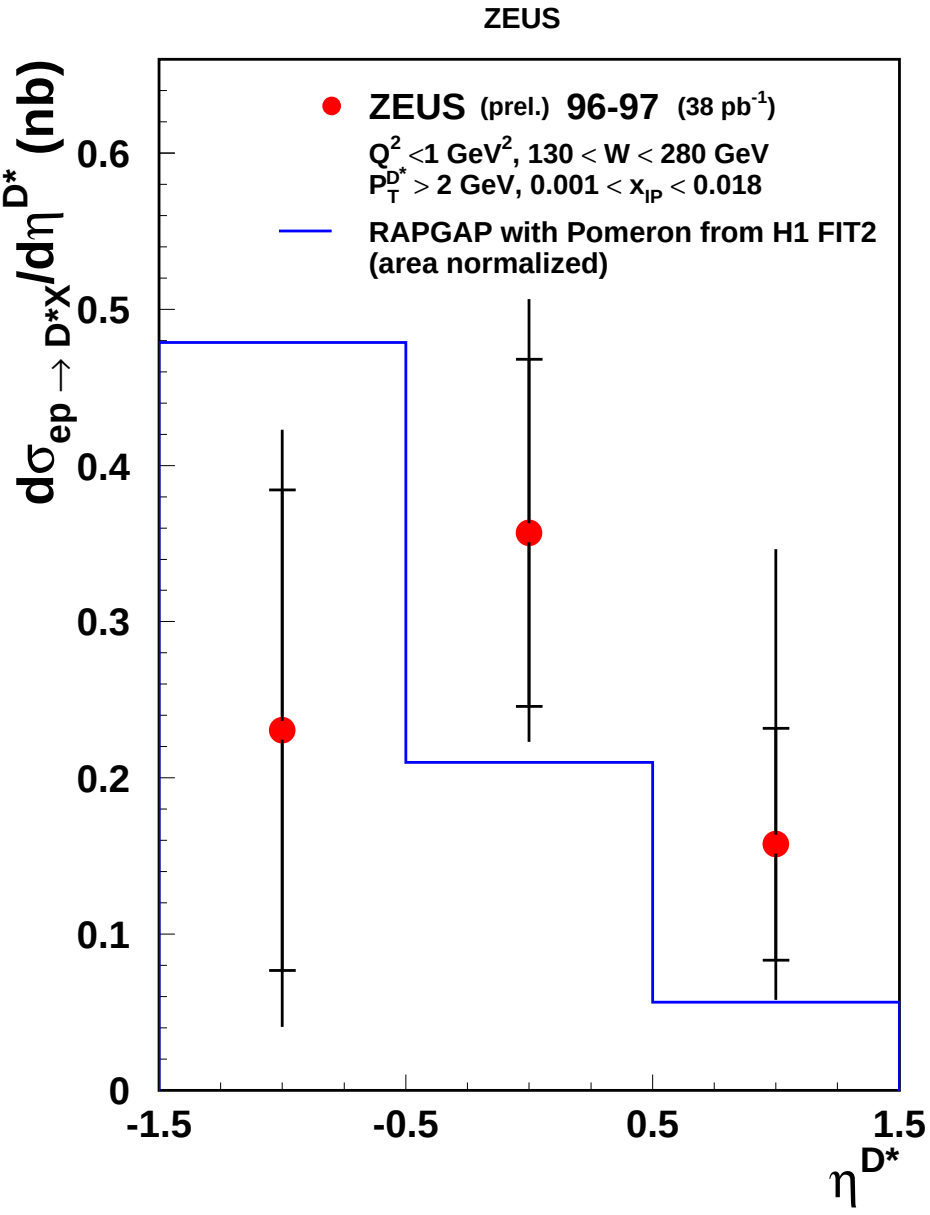

Figure 4: *Differential cross section $d\sigma/d\eta^{D^*}$ (dots) for the diffractive photoproduction reaction $ep \to e' D^* X p'$ for $Q^2 < 1\ GeV^2$, $130 < W < 280\ GeV$ and $0.001 < x_{I\!P} < 0.18$. The kinematic range of measurements is $p_T^{D^*} > 2\ GeV$ and $|\eta^{D^*}| < 1.5$. The inner bars show the statistical errors, and the outer bars correspond to thestatistical and systematic errors, added in quadrature. The data are compared with the distributions of the RAPGAP MC diffractive events, simulated in the framework of the resolved Pomeron model with the H1 FIT2 Pomeron parametrization (histogram). The MC distribution has been normalized to have the same area as the data distribution.*

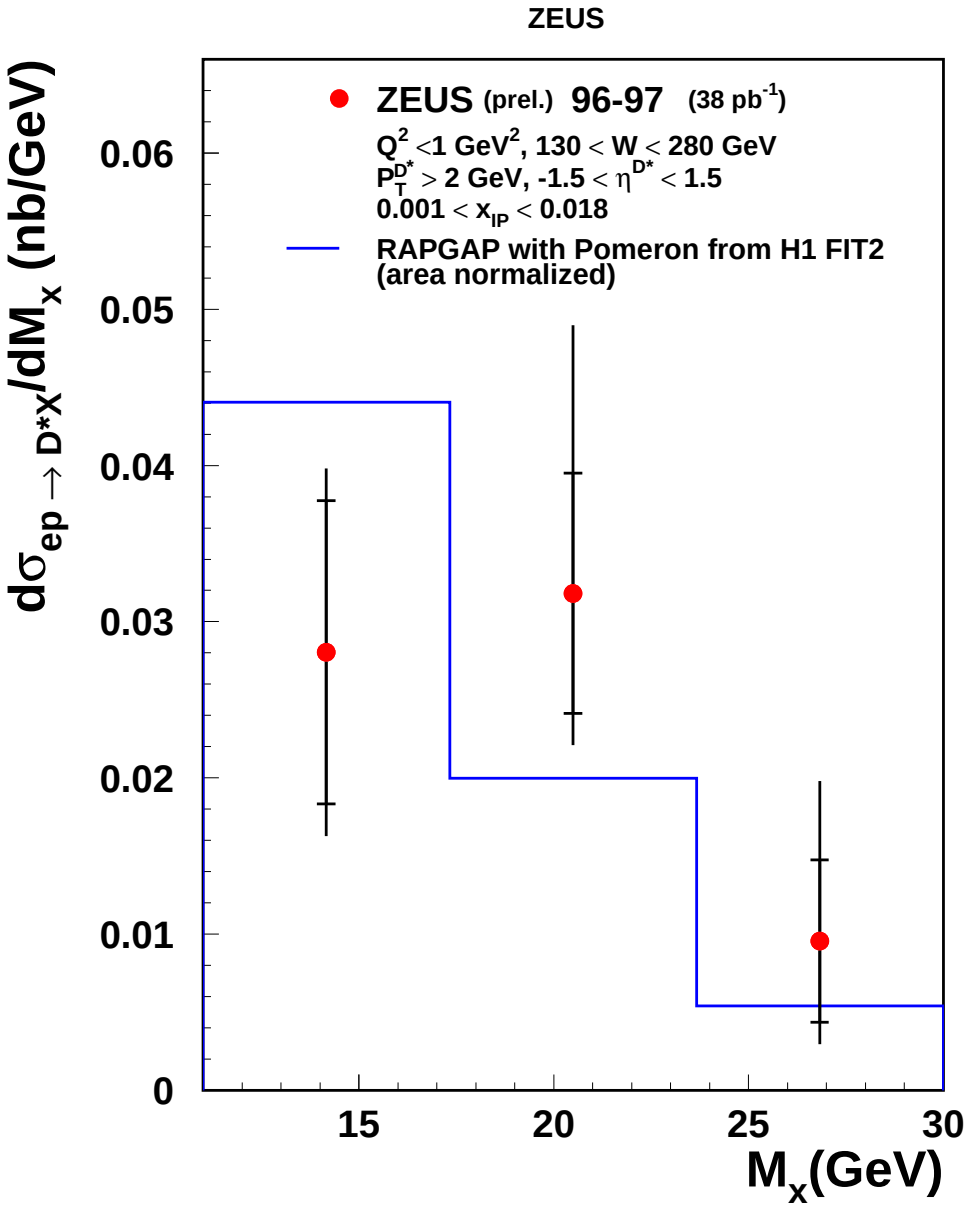

Figure 5: *Differential cross section $d\sigma/dM_X$ (dots) for the diffractive photoproduction reaction $ep \to e' D^* X p'$ for $Q^2 < 1\ GeV^2$, $130 < W < 280\ GeV$ and $0.001 < x_{I\!P} < 0.18$. The kinematic range of measurements is $p_T^{D^*} > 2\ GeV$ and $|\eta^{D^*}| < 1.5$. The inner bars show the statistical errors, and the outer bars correspond to thestatistical and systematic errors, added in quadrature. The data are compared with the distributions of the RAPGAP MC diffractive events, simulated in the framework of the resolved Pomeron model with the H1 FIT2 Pomeron parametrization (histogram). The MC distribution has been normalized to have the same area as the data distribution.*

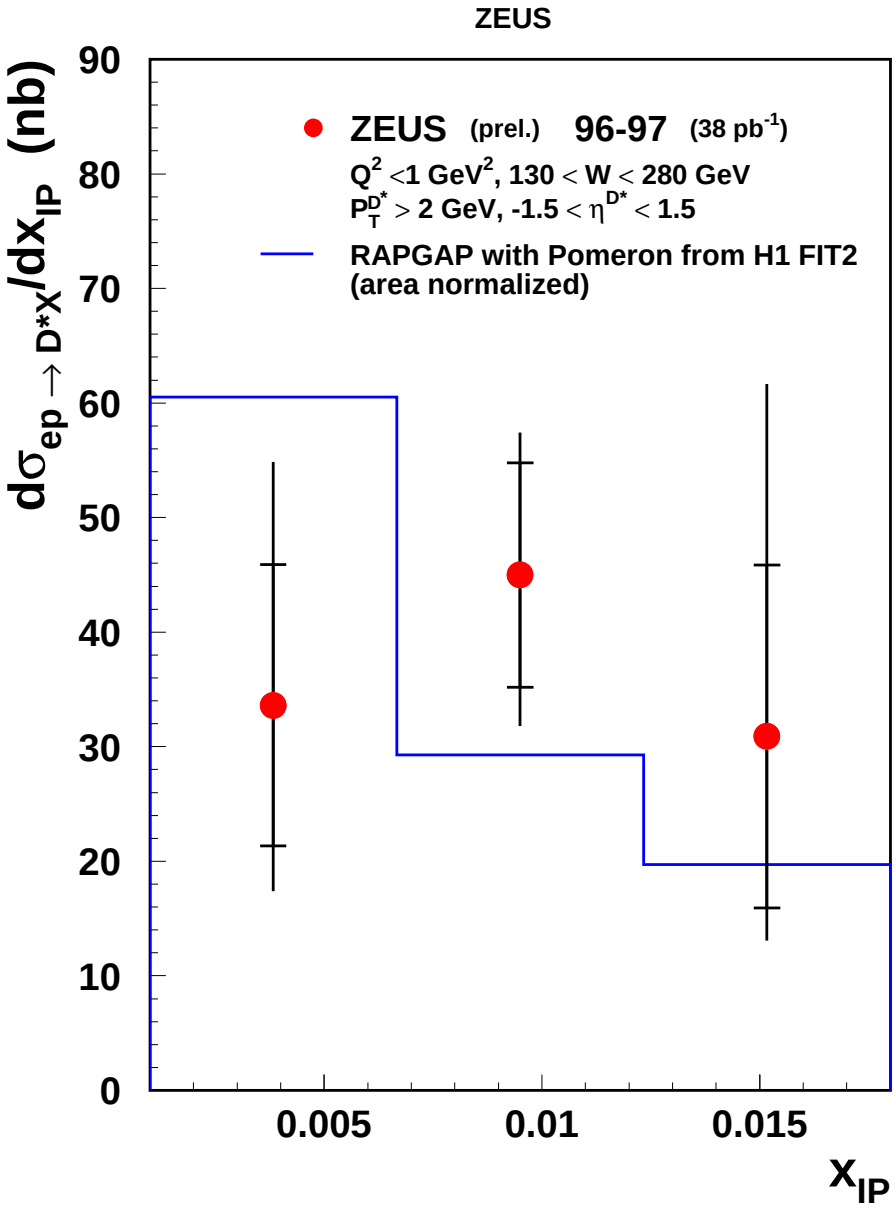

Figure 6: *Differential cross section $d\sigma/dx_{I\!P}$ (dots) for the diffractive photoproduction reaction $ep \to e' D^* X p'$ for $Q^2 < 1\ GeV^2$, $130 < W < 280\ GeV$ and $0.001 < x_{I\!P} < 0.18$. The kinematic range of measurements is $p_T^{D^*} > 2\ GeV$ and $|\eta^{D^*}| < 1.5$. The inner bars show the statistical errors, and the outer bars correspond to the statistical and systematic errors, added in quadrature. The data are compared with the distributions of the RAPGAP MC diffractive events, simulated in the framework of the resolved Pomeron model with the H1 FIT2 Pomeron parametrization (histogram). The MC distribution has been normalized to have the same area as the data distribution.*